2014-09

Charge Collection in Bulk Heterojunction Organic Photovoltaic Devices

UTD AUTHOR(S): Liang Xu, Yun-Ju Lee and Julia W. P. Hsu

Aad, G., B. Abbott, J. Abdallah, S. Abdel Khalek, et al. 2014. "Search for squarks and gluinos with the ATLAS detector in final states with jets and missing transverse momentum using √s = 8 TeV proton-proton collision data." Journal of High Energy Physics 2014(176): 1-52.

Charge collection in bulk heterojunction organic photovoltaic devices: An impedance spectroscopy study

Liang Xu, Yun-Ju Lee, and Julia W. P. Hsu[a)]
Department of Materials Science and Engineering, University of Texas at Dallas, Richardson, Texas 75080, USA

(Received 16 July 2014; accepted 15 September 2014; published online 24 September 2014)

Through thickness and applied bias variation, charge collection in poly(3-hexylthiophene):[6,6]-phenyl C61-butyric acid methyl ester (P3HT:PCBM) bulk heterojunction organic photovoltaic (OPV) devices was investigated with impedance spectroscopy. An equivalent circuit model incorporating chemical capacitance (C_μ), recombination resistance (R_2), and transport resistance (R_1) was used to analyze the results. Insufficient carrier extraction, exhibiting diffusion transport characteristics at high frequencies, was found in devices with a thick active layer. These devices also display a higher chemical capacitance, indicating greater carrier accumulation, and a lower recombination resistance, signaling increased bimolecular recombination. Increasing internal field with negative applied bias enhances carrier collection by reducing carrier accumulation and recombination. Moreover, we showed explicitly that charge collection can be quantified by $(R_2/R_1)^{1/2}$, which is proportional to device fill factor. These results demonstrate that impedance spectroscopy is an effective tool for investigating charge collection in OPV devices. © *2014 AIP Publishing LLC*. [http://dx.doi.org/10.1063/1.4896633]

Efficient energy conversion in organic photovoltaic (OPV) requires the combination of high generation and collection of carriers. The bulk heterojunction (BHJ) structure consisting of percolated domains of electron donor and electron acceptor with characteristic domain size comparable to the exciton diffusion length is used to facilitate exciton dissociation and maximize carrier generation efficiency.[1,2] The photogenerated charge carriers then transport to respective electrodes, driven predominately by the built-in electric field. However, bimolecular recombination during carrier transport can be significant.[3,4] Therefore, charge collection, i.e., competition between carrier sweep-out by the internal field and the loss of photogenerated carriers through recombination, must be quantified to increase the efficiency of BHJ OPV devices.

Impedance spectroscopy (IS) is a powerful, non-destructive characterization tool to study frequency-dependent behavior that yield useful information about the physicochemical properties of a wide variety of electronic devices.[5–8] Analysis of IS data taken over a broad frequency range (10^{-3}–10^{6} Hz) can discern processes that occur at different time scales within one system. Recently, impedance analysis has been applied to OPV devices to obtain average charge carrier lifetime, electronic density of states, and charge carrier concentrations.[9–11] At open circuit condition, carrier recombination is dominant and the analysis is simplified.[10,11] For other bias conditions, where charge extraction and recombination compete with each other, the analysis is more complicated and a clear understanding of impedance analysis is still lacking.

Various studies have shown that OPV device performance depends on active layer thickness in a complex manner.[3,12–14] It is evident that the absorption of photons can be enhanced by increasing the thickness of the active layer. However, as the active layer thickness increases, the path lengths of photogenerated electrons and holes to their corresponding electrodes increase, which dramatically reduce charge collection efficiency.[3,14] Moreover, asymmetric transport properties including unintentional doping,[13] unbalanced electron and hole mobilities[3,14–16] can significantly modify the internal field and affect charge carrier dynamics. Here, we perform IS on inverted poly(3-hexylthiophene):[6,6]-phenyl C61-butyric acid methyl ester (P3HT:PCBM) BHJ OPV devices of different active layer thicknesses, and identify their difference in charge dynamics through equivalent circuit analysis of the IS results. Specifically, carrier accumulation and recombination are analyzed separately in terms of chemical capacitance and recombination resistance, respectively, obtained from IS analysis. We determine the relationship between the resistance and capacitance values of the equivalent circuit as a function of active layer thickness and bias. Moreover, we identify the ratio of recombination resistance and transport resistance, which strongly correlates to device fill factor (FF), as the key parameter to quantify carrier collection efficiency. Thus, IS analysis is able to explicitly reveal carrier collection information.

The inverted device architecture consists of ITO cathode, ZnO electron transport layer, P3HT:PCBM (80 nm–325 nm thickness), MoO_3 hole transport layer, and Ag anode. Detailed device recipe has been published previously.[17] The current density–voltage (J–V) curves were measured in N_2 under a class AAA solar simulator (Abet Technologies Sun 3000) with an AM 1.5G filter at 100 mW/cm^2 using a low noise source meter (Keithley 2635 A). The solar simulator intensity was set using a NIST-traceable calibrated photodiode (Abet RR_227 KG5). The impedance measurements were carried out in a O-ring sealed sample holder containing N_2 at room temperature, using a Zahner IM6 electrochemical workstation

[a)]Author to whom correspondence should be addressed. Electronic mail: jwhsu@utdallas.edu

with the frequency range between 1 Hz and 1 MHz, illuminated by a white light emitting diode (Zahner WLC01) with intensity of 70 mW/cm^2 controlled by a power source (Zahner PP211), and with DC bias ranging from −2 V to 0.4 V. The AC bias amplitude was 20 mV to maintain the linear response. Equivalent circuit modeling was optimized with software ZMAN 2.0.

Fig. 1(a) shows the J-V curves for four devices of increasing thicknesses, which exhibit a monotonic decrease in the fill factor and the open circuit voltage (V_{oc}). Device parameters are given in Table SI.[33] These trends are consistent with results from published literature and are attributed to the less effective charge collection in thick active layer devices.[3,12–14] Nyquist plots of different thickness devices measured at 0 V DC bias (SC condition) under 70 mW/cm^2 white light LED illumination (equivalent to AM 1.5G 100 mW/cm^2 illumination calibrated by Abet RR_227 KG5 photodiode) are shown in Fig. 1(b). The Nyquist plots for all samples consist of two semicircles at different frequency regions: Fig. 1(b) shows the high-frequency responses, while Fig. 1(b) inset shows the low-frequency semicircles. As device thickness increases, the low-frequency semicircle decreases in diameter and the high-frequency semicircle becomes more prominent. The dashed line in Fig. 1(b) shows the 45° slope, which is a fingerprint of diffusive transport (Warburg response).[18] It is clear that, even at 0 V bias condition, charge collection is inefficient for the 225 nm and 325 nm devices, as indicated by the diffusive transport.

These IS data were modeled by the equivalent circuit shown in Fig. 1(c) to identify the underlying physical parameters: a series resistance R_s, a transport resistance R_1, a device capacitance C_1 associated with the depletion region within the active layer, and a recombination resistance R_2 in parallel with a constant phase element (CPE).[9] The R_s is the resistance from contact layers and electrodes. The $R_1 \,||\, C_1$ combination contributes to the high-frequency region of the impedance response in the Nyquist plot, while the $R_2 \,||$ CPE combination is associated with the internal charge transfer events including accumulation (CPE) and recombination (R_2) and contributes to the low-frequency response.[9,19,20] CPE is used to describe the inhomogeneous nature of BHJ active layer that exhibits a distribution of relaxation times with impedance $Z_{CPE} = Y_0^{-1}(j\omega)^{-n}$, where Y_0 is the coefficient of the CPE and n represents an "ideality" factor characteristic of the distribution of relaxation times.[21,22] As shown in Fig. 1(b), this equivalent circuit provides a high quality fit of the data over the entire frequency range of the measurement. All fitting parameters are given in Table SII.[33] Moreover, such equivalent circuit is a versatile model and can be simplified at open- and short-circuit conditions. At open circuit ($V = V_{oc}$), the depletion region collapses making C_1 vanish (the circuit is open at C_1 position); therefore, R_1 becomes part of the series resistance and the equivalent circuit evolves to a circuit of $R_2 \,||$ CPE in series with $R_s + R_1$, which is widely used in impedance analysis at open circuit condition.[10,11] On the other hand, under a condition of effective charge collection as well as in dark (no carrier generation), there will be no additional charge accumulation. As a result, we can neglect CPE and the equivalent circuit becomes $R \,||\, C_1$ in series with R_s, where $R = R_1 + R_2$. This is consistent with the observation that for the thin device (Fig. 1(b), red) as well as device at large negative bias (Fig. 2(a), black) the impedance response is almost one semicircle.

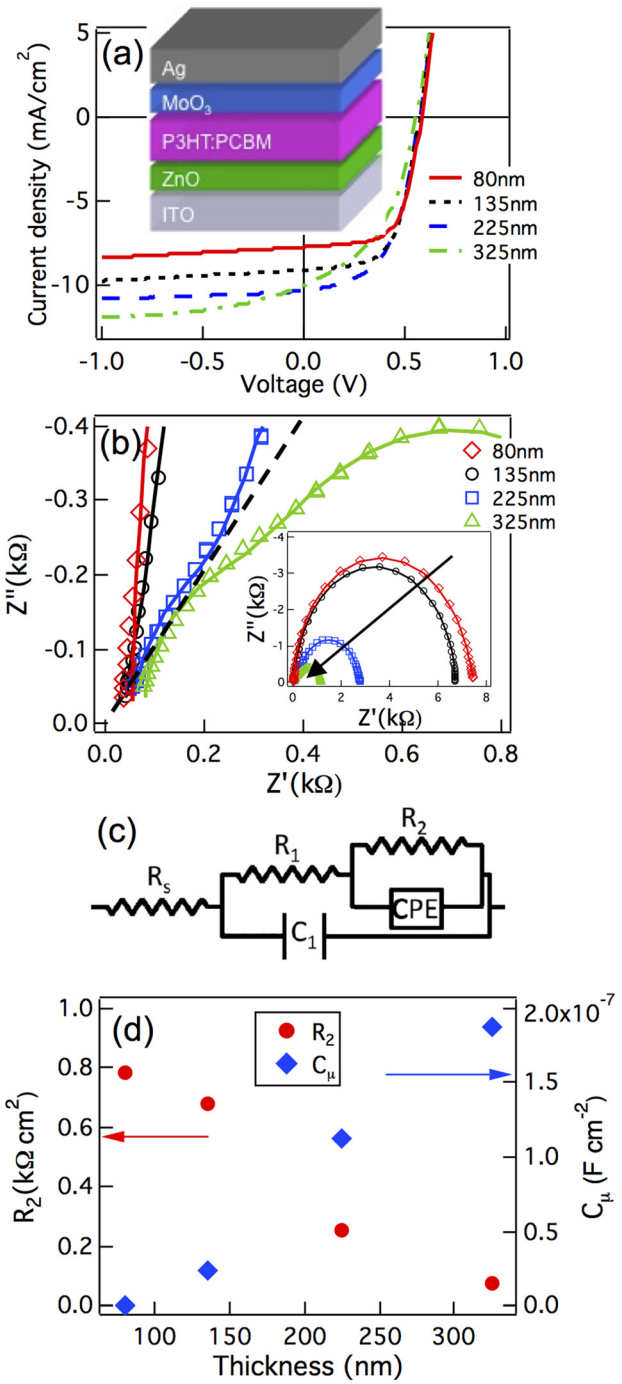

FIG. 1. (a) J-V curves taken at AM 1.5G 100 mW/cm^2 illumination condition of inverted P3HT:PCBM BHJ solar cells with different active layer thicknesses: 55 nm (solid), 135 nm (dotted), 225 nm (dashed), and 325 nm (dashed-dotted). (b) Impedance response of inverted P3HT:PCBM BHJ solar cells with different active layer thicknesses (diamonds for 55 nm, circles for 135 nm, squares for 225 nm, and triangles for 325 nm) at 0 V sample bias and 70 mW/cm^2 illumination intensity. The dashed line is the 45° slope in the Nyquest plot; thicker devices exhibit this feature in the high-frequency response. The arrow indicates increasing active layer thickness. The color scheme for the different thicknesses is the same as (a). (c) Equivalent circuit used to analyze IS data shown in (b). The solid lines in (b) are fits to experimental data using the equivalent circuit. (d) R_2 (circles) and C_μ (diamonds) vs. active layer thickness extracted from the fitting data in (b) to the equivalent circuit in (c).

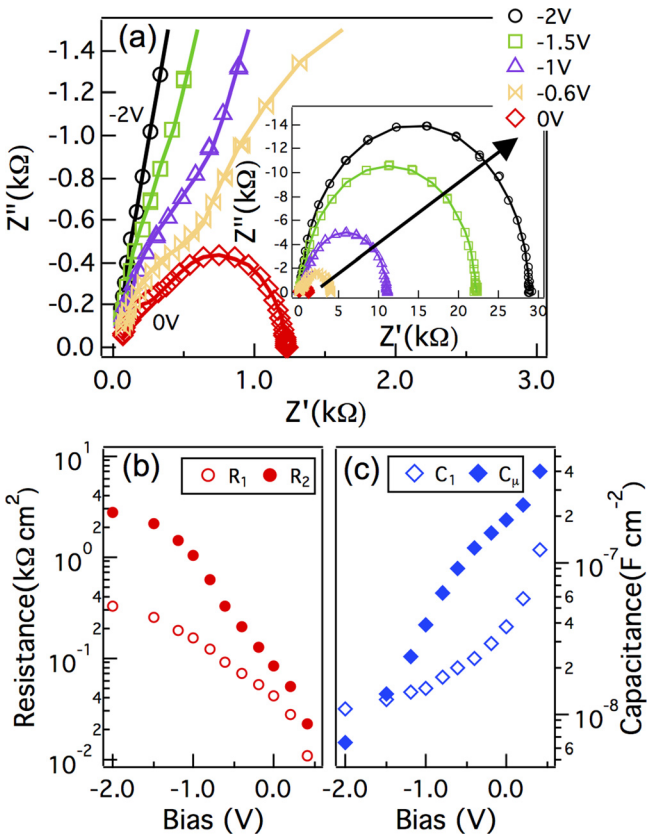

FIG. 2. Impedance results for inverted P3HT:PCBM BHJ solar cell with active layer thickness of 325 nm under 70 mW/cm^2 illumination intensity with different applied bias: −2 V (circles), −1.5 V (squares), −1 V (triangles), −0.6 V (butterflies), and 0 V (diamonds). (a) Impedance response to applied bias varying from 0 to −2 V. The arrow indicates increasing negative bias. The solid lines are the fitting results. (b) R_1 (open circles) and R_2 (solid circles) vs. applied bias voltage from fitting data shown in (a). (c) C_1 (open diamonds) and C_μ (solid diamonds) vs. applied bias voltage from fitting data shown in (a).

Fig. 1(d) shows R_2 and C_μ extracted from fitting the impedance response at 0 V bias of different-thickness P3HT:PCBM devices. The chemical capacitance C_μ, which reflects carrier accumulation inside active layer,[23] is calculated by using the equation

$$C_\mu = \frac{(Y_0 R_2)^{\frac{1}{n}}}{R_2}, \quad (1)$$

where Y_0 and n are the two parameters of CPE obtained from equivalent circuit fitting. Physically, the accumulated photogenerated carriers that increase C_μ have two ways to escape: collected through the external pathway in terms of photocurrent or recombined through the recombination resistor (R_2).[23] We note that a larger R_2 indicates a greater resistance to carrier recombination.[23] At 0 V bias, we can see from Fig. 1(d) that C_μ increases and R_2 decreases monotonically with increasing active layer thickness. Such an increase in carrier accumulation and recombination in thick devices can be explained by the decreased extraction efficiency due to weaker internal field and longer transport path, which results in more carriers accumulated inside the active layer and thus higher bimolecular recombination.[24,25] Additionally, C_1 decreases and then flattens out as the thickness increases (Fig. S1),[33] suggesting that for thicker active layer devices, the depletion region is limited to a constant thickness that is smaller than the active layer thickness. This is consistent with published drift-diffusion simulation results, which show that thinner active layers are fully depleted, while the thicker active layers contain a field-free region far away from the electrodes.[13] The diffusive transport behavior observed for thick devices in Fig. 1(b) results from the presence of the field-free region.[26]

The previous section shows that, at 0 V bias condition, as active layer thickness increases, inefficient charge collection, which manifests in a diffusive transport (45° slope of the high-frequency response), causes carriers to accumulate inside the active layer (higher C_μ) and recombine (lower R_2). To further verify the finding, we performed IS measurements on the thickest (325 nm) device at 70 mW/cm^2 illumination intensity under different voltage biases. We used the same equivalent circuit to fit all data. As the bias goes from +0.4 V to −2 V, the low-frequency semicircle becomes larger (Fig. 2(a) inset) and the diffusive transport fingerprint at high frequencies become less obvious (Fig. 2(a)). From the fitting results, C_1 (Fig. 2(c), open) and C_μ (Fig. 2(c), solid) decrease and R_1 (Fig. 2(b), open) and R_2 (Fig. 2(b), solid) increase with more negative bias. The fit parameters are summarized in Table SIII.[33] Since carrier generation is the same under different biases,[27] a negative bias increases the drift field across the active layer[19] and at the same time decreases the field-free region (a wider depletion region). Therefore, carriers are more efficiently collected by the external circuit instead of recombining, leading to a smaller C_μ and larger R_2. The widening of depletion region inside active layer by applying negative bias is also evident by the decrease of C_1 and increase of R_1. We note that at −2 V bias, C_1 saturated at 1.1 nF. If we assume a fully depleted active layer with thickness of 325 nm and device area of 0.11 cm^2, this corresponds to a dielectric constant of 3.6 for the P3HT:PCBM blend, which falls within the range of previously reported values determined by other techniques.[28,29] Thus, the IS results under different applied bias values support our interpretation of R_1, R_2, C_1, and C_μ.

To demonstrate that impedance study of charge collection can be correlated to device performance, we investigate the competition between transport and recombination in different thickness devices at 0 V bias condition. In the equivalent circuit used here, the slowest transport time is the diffusion time determined by the transport resistance and the chemical capacitance, i.e., R_1C_μ, while the electron recombination time is determined by the recombination resistance and the chemical capacitance, i.e., R_2C_μ. We can then obtain characteristic length scales for these two mechanisms through $L^2 = D_n R_1 C_\mu$ and $L_n^2 = D_n R_2 C_\mu$, where D_n is the electron diffusion coefficient, L is the active layer thickness, and L_n is the electron diffusion length.[26,30] The key parameter that affects the carrier collection efficiency is the ratio of L_n to L, which equals $(R_2/R_1)^{1/2}$. For $L_n/L \gg 1$, i.e., thin devices, the photogenerated carriers can be efficiently collected, while carriers are not able to reach the electrodes for devices with $L_n/L \ll 1$. As shown in Fig. 3, $(R_2/R_1)^{1/2}$ strongly correlates with FF obtained from J-V measurements, which represents the collection efficiency for photogenerated carriers.[31,32] For the thicker devices in this study, $L_n/L \sim 1$, which means diffusive transport becomes important due to weaker internal field as well as

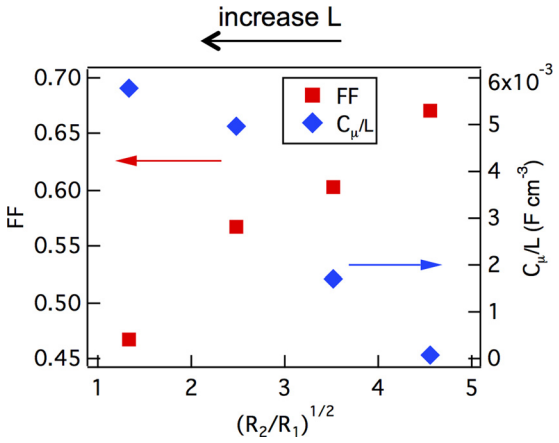

FIG. 3. FF (squares) and C_μ/L (diamonds) vs. $(R_2/R_1)^{1/2}$ at SC condition under 70 mW/cm^2 illumination for inverted P3HT:PCBM BHJ solar cells with different active layer thickness.

larger field-free region inside the active layer. Consequently, charge collection is reduced and devices show a lower FF. Moreover, chemical capacitance, by definition, is the capability of a system to accept or release additional carriers with density n due to a change in their chemical potential μ,[26]

$$C_\mu = q^2 L \frac{dn}{d\mu}, \tag{2}$$

where q is the magnitude of elementary charge. If we assume that photogenerated carrier density is low at 0 V bias condition (short-circuit condition), n would obey Boltzmann distribution, and C_μ/L is proportional to photogenerated carrier density. Therefore, inefficient carrier collection in thick devices, which is represented by a smaller value of $(R_2/R_1)^{1/2}$ also results in a higher carrier density inside the device, as shown by the inverse correlation between $(R_2/R_1)^{1/2}$ and C_μ/L in Fig. 3. Overall, carrier collection can be quantified by $(R_2/R_1)^{1/2}$ from the impedance analysis at 0 V bias conditions.

In summary, we perform impedance spectroscopy on P3HT:PCBM OPV devices of different BHJ active layer thicknesses over a range of applied biases. An equivalent circuit, consisting of a series resistance, a transport resistance, a device capacitance, a recombination resistance, and a CPE, is used to identify the underlying physical mechanisms. We show that quantitative information on carrier accumulation and recombination can be obtained from examining C_μ and R_2, respectively. At different operating conditions, carrier collection efficiency is the balance of carrier accumulation, indicated by C_μ, and carrier recombination, reflected by R_2. We demonstrate that devices thicker than optimal exhibit a field-free region and diffusive transport, leading to inefficient carrier collection and significant carrier accumulation inside the devices. Specifically, we show that at 0 V bias condition $(R_2/R_1)^{1/2}$ is related to charge collection efficiency in OPV devices, which is proportional to the fill factor and inversely correlated to carrier density.

We would like to thank Jian Wang for useful discussion and Diego Barrera for help with sample preparation. This project is supported by the University of Texas at Dallas and National Science Foundation DMR-1305893. J.W.P.H. acknowledges the Texas Instruments Distinguished Chair in Nanoelectronics.

[1]G. Yu, J. Gao, J. C. Hummelen, F. Wudl, and A. J. Heeger, Science **270**, 1789 (1995).
[2]L. Dou, J. You, Z. Hong, Z. Xu, G. Li, R. A. Street, and Y. Yang, Adv. Mater. **25**, 6642 (2013).
[3]S. R. Cowan, J. Wang, J. Yi, Y.-J. Lee, D. C. Olson, and J. W. P. Hsu, J. Appl. Phys. **113**, 154504 (2013).
[4]L. J. A. Koster, M. Kemerink, M. M. Wienk, K. Maturová, and R. A. J. Janssen, Adv. Mater. **23**, 1670 (2011).
[5]I. Mora-Seró, J. Bisquert, F. Fabregat-Santiago, G. Garcia-Belmonte, G. Zoppi, K. Durose, Y. Proskuryakov, I. Oja, A. Belaidi, and T. Dittrich, Nano Lett. **6**, 640 (2006).
[6]V. González-Pedro, X. Xu, I. Mora-Seró, and J. Bisquert, ACS Nano **4**, 5783 (2010).
[7]J. Bisquert, D. Cahen, G. Hodes, S. Rühle, and A. Zaban, J. Phys. Chem. B **108**, 8106 (2004).
[8]I. H. Campbell, D. L. Smith, and J. P. Ferraris, Appl. Phys. Lett. **66**, 3030 (1995).
[9]B. J. Leever, C. A. Bailey, T. J. Marks, M. C. Hersam, and M. F. Durstock, Adv. Energy Mater. **2**, 120 (2012).
[10]F. Fabregat-Santiago, G. Garcia-Belmonte, I. Mora-Seró, and J. Bisquert, Phys. Chem. Chem. Phys. **13**, 9083 (2011).
[11]G. Garcia-Belmonte, P. P. Boix, J. Bisquert, M. Sessolo, and H. J. Bolink, Sol. Energy Mater. Sol. Cells **94**, 366 (2010).
[12]M. Lenes, L. J. A. Koster, V. D. Mihailetchi, and P. W. M. Blom, Appl. Phys. Lett. **88**, 243502 (2006).
[13]T. Kirchartz, T. Agostinelli, M. Campoy-Quiles, W. Gong, and J. Nelson, J. Phys. Chem. Lett. **3**, 3470 (2012).
[14]T. J. K. Brenner, Y. Vaynzof, Z. Li, D. Kabra, R. H. Friend, and C. R. McNeill, J. Phys. D: Appl. Phys. **45**, 415101 (2012).
[15]L. J. A. Koster, V. D. Mihailetchi, H. Xie, and P. W. M. Blom, Appl. Phys. Lett. **87**, 203502 (2005).
[16]V. Mihailetchi, J. Wildeman, and P. Blom, Phys. Rev. Lett. **94**, 126602 (2005).
[17]D. Barrera, Y.-J. Lee, and J. W. P. Hsu, Sol. Energy Mater. Sol. Cells **125**, 27 (2014).
[18]T. Ripolles-Sanchis, A. Guerrero, J. Bisquert, and G. Garcia-Belmonte, J. Phys. Chem. C **116**, 16925 (2012).
[19]J. Bisquert and G. Garcia-Belmonte, J. Phys. Chem. Lett. **2**, 1950 (2011).
[20]A. Guerrero, S. Loser, G. Garcia-Belmonte, C. J. Bruns, J. Smith, H. Miyauchi, S. I. Stupp, J. Bisquert, and T. J. Marks, Phys. Chem. Chem. Phys. **15**, 16456 (2013).
[21]E. Barsoukov and J. R. Macdonald, *Impedance Spectroscopy* (John Wiley & Sons, 2005).
[22]C. H. Hsu and F. Mansfeld, Corrosion **57**, 747 (2001).
[23]J. Bisquert, Phys. Chem. Chem. Phys. **5**, 5360 (2003).
[24]C. G. Shuttle, B. O'Regan, A. M. Ballantyne, J. Nelson, D. D. C. Bradley, J. de Mello, and J. R. Durrant, Appl. Phys. Lett. **92**, 093311 (2008).
[25]C. Shuttle, B. O'Regan, A. Ballantyne, J. Nelson, D. Bradley, and J. Durrant, Phys. Rev. B **78**, 113201 (2008).
[26]G. Garcia-Belmonte, A. Guerrero, and J. Bisquert, J. Phys. Chem. Lett. **4**, 877 (2013).
[27]R. A. Street, S. Cowan, and A. J. Heeger, Phys. Rev. B **82**, 121301 (2010).
[28]J. Schafferhans, A. Baumann, A. Wagenpfahl, C. Deibel, and V. Dyakonov, Org. Electron. **11**, 1693 (2010).
[29]C. Deibel, A. Wagenpfahl, and V. Dyakonov, Phys. Status Solidi RRL **2**, 175 (2008).
[30]J. Bisquert and I. Mora-Seró, J. Phys. Chem. Lett. **1**, 450 (2010).
[31]B. Qi and J. Wang, Phys. Chem. Chem. Phys. **15**, 8972 (2013).
[32]B. Chen, X. Qiao, C.-M. Liu, C. Zhao, H.-C. Chen, K.-H. Wei, and B. Hu, Appl. Phys. Lett. **102**, 193302 (2013).
[33]See supplementary material at http://dx.doi.org/10.1063/1.4896633 for transport resistance (R1) and device capacitance (C1) vs. active layer thickness extracted from the equivalent circuit fitting, device parameters measured from J-V measurement under AM 1.5G one-sun (100 mW/cm2) illumination condition, equivalent circuit fitting parameters of devices with different active layer thickness and applied bias.